

HEAT TRANSFER FOR MHD FLOW THROUGH A RECTANGULAR PIPE WITH DISCONTINUITY IN WALL TEMPERATURES

BANI SINGH

Department of Mathematics, University of Roorkee, Roorkee, U.P., India

and

JIA LAL

Roorkee University Regional Computer Centre, Roorkee, U.P., India

(Received 5 May 1981 and in final form 12 January 1982)

Abstract—The temperature distribution for steady MHD axial flow through a rectangular pipe has been calculated numerically. Owing to the discontinuity in the wall temperatures, the resulting differential equation which is a 3-dim. elliptic partial differential equation with variable coefficients, becomes impossible to handle analytically. The traditional finite difference methods become unsuitable due to the very large number of unknowns involved. The ADI method is found to be most suitable for the problem as it saves time as well as computer storage. Graphs are given to depict the temperature distribution near and away from the discontinuity for various Hartmann numbers.

NOMENCLATURE

c ,	specific heat;
\bar{V}, V ,	velocity;
B_0 ,	applied magnetic field;
B ,	induced magnetic field;
Pe ,	Peclet number;
k ,	thermal conductivity;
J ,	current density;
$-K$,	pressure gradient;
M ,	Hartmann number;
x', y', z' ,	space coordinates;
x, y, z ,	nondimensional space coordinates;
a, b, T_1, T_2 ,	arbitrary constants.

Greek symbols

θ', θ ,	temperature;
η ,	coefficient of viscosity;
ρ ,	density;
σ ,	electrical conductivity;
ω ,	a parameter;
μ_0 ,	a constant;
$\delta_x, \delta_y, \delta_z$,	central difference operators;
μ_z ,	mean difference operator;
$\Delta x, \Delta y, \Delta z$,	space intervals in x, y and z directions, respectively;
β ,	reciprocal of Peclet number;
Φ ,	dissipation function.

Subscripts

I, J, K ,	represent order of the matrices;
i, j, k ,	location in (x, y, z) space.

Superscripts

n ,	number of iterations;
$*, **$,	intermediate levels between two con- secutive iterations.

1. INTRODUCTION

HEAT transfer for MHD flow between parallel plates when the temperature on one side ($z < 0$) is different from the other side ($z > 0$), was considered by Nigam and Singh [1]. Singh and Lal [2] considered a similar problem for heat transfer for MHD flow between two coaxial cylinders.

In this paper, we discuss the solution for the temperature distribution in the flow region of a rectangular pipe when there is a temperature discontinuity in the wall temperatures at a given section. The walls are assumed to be of nonconducting material and the applied magnetic field is transverse and parallel to a side of the section (Fig. 1). The x' -axis is parallel to the applied magnetic field B_0 , y' -axis perpendicular to it and in the section and the z' -axis along the flow direction. The boundary temperature has a discontinuity at the section $z' = 0$, to the left of which the boundary temperature is T_1 while to the right it is T_2 . The aim is to compute the temperature distribution in the region $-a < x' < a$, $-b < y' < b$ and $-\infty < z' < \infty$, where $2a$ and $2b$ are the sides of the section.

For large values of $|z'|$, the perturbations due to the discontinuity at $z' = 0$ are negligible and the problem reduces to a simple 2-dim. Dirichlet problem, the solution of which has been found by the finite difference method. But in the vicinity of $z' = 0$ the situation becomes complicated owing to the involvement of all the three space variables. The usual finite difference method becomes too uneconomical due to the very large number of unknowns involved. We have found that for this problem the alternating direction implicit (ADI) method is very efficient and economical. It reduces the problem to one of solving tridiagonal systems of equations alternately along lines parallel to axes, thereby sufficiently reducing the number of

unknowns to be found at one time. The results were obtained for various Hartmann numbers in the entire flow region. They are discussed for selected points and lines and graphs are drawn to show their behaviour along some of these lines.

2. BASIC EQUATIONS

The energy equation for MHD flows is

$$\rho c(\vec{V} \cdot \nabla)\theta' = \Phi + k\nabla^2\theta' + J^2/\sigma. \quad (1)$$

In cartesian co-ordinates (x', y', z'), equation (1) becomes

$$\begin{aligned} \rho c V_{z'} \frac{\partial \theta'}{\partial z'} = & \eta \left[\left(\frac{\partial V_{z'}}{\partial y'} \right)^2 + \left(\frac{\partial V_{z'}}{\partial x'} \right)^2 \right] \\ & + \frac{1}{\mu_0^2 \sigma} \left[\left(\frac{\partial B_{z'}}{\partial y'} \right)^2 + \left(\frac{\partial B_{z'}}{\partial x'} \right)^2 \right] \\ & + k \left[\frac{\partial^2 \theta'}{\partial x'^2} + \frac{\partial^2 \theta'}{\partial y'^2} + \frac{\partial^2 \theta'}{\partial z'^2} \right]. \end{aligned} \quad (2)$$

The boundary conditions on θ' are

$$\begin{aligned} \theta'(\pm a, y', z') &= T_1, \quad |y'| \leq b, \quad z' < 0, \\ \theta'(x', \pm b, z') &= T_1, \quad |x'| \leq a, \quad z' < 0, \\ \theta'(\pm a, y', z') &= T_2, \quad |y'| \leq b, \quad z' > 0, \\ \theta'(x', \pm b, z') &= T_2, \quad |x'| \leq a, \quad z' > 0. \end{aligned} \quad (3)$$

To nondimensionalize equation (2) we introduce the following nondimensional variables and parameters:

$$\begin{aligned} \theta &= (\theta' - T_2)/(T_1 - T_2), \\ x &= x'/a, \quad y = y'/a, \quad \chi = b/a, \\ V_0 &= Ka^2/\eta, \quad V = V_z/V_0, \quad -K = \text{pressure gradient}, \\ P_e &= V_0 a c/k = \text{Peclet number}, \quad \beta = 1/P_e, \\ B &= B_z/[V_0 \mu_0 (\sigma \eta)^{1/2}], \\ z &= z'/(a P_e), \\ Q &= \eta V_0^2/[k(T_1 - T_2)], \\ M &= B_0 a (\sigma/\eta)^{1/2} = \text{Hartmann number}. \end{aligned} \quad (4)$$

Then equation (2) takes the form

$$\nabla^2 \theta + \beta^2 \frac{\partial^2 \theta}{\partial z^2} = V(x, y) \frac{\partial \theta}{\partial z} - Q[(\nabla V)^2 + (\nabla B)^2] \quad (5)$$

where

$$\nabla^2 = \frac{\partial^2}{\partial x^2} + \frac{\partial^2}{\partial y^2}.$$

Notice that V and B are functions of x and y only. This is due to the assumption that the buoyancy forces caused by the temperature difference are negligible as compared to the inertial and frictional forces. The same assumption is made by Nigam and Singh [1] for the problem of Hartmann flow. Singh and Lal [2] have solved a similar problem for the flow between two coaxial cylinders under radial magnetic field. This assumption implies that the expressions for V and B may be taken from previous papers that have dealt with the determination of V and B .

The boundary conditions now become

$$\begin{aligned} \theta(\pm 1, y, z) &= 1, \quad |y| < \chi, \quad z < 0, \\ \theta(x, \pm \chi, z) &= 1, \quad |x| < 1, \quad z < 0, \\ \theta(\pm 1, y, z) &= 0, \quad |y| < \chi, \quad z > 0, \\ \theta(x, \pm \chi, z) &= 0, \quad |x| < 1, \quad z > 0. \end{aligned} \quad (6)$$

When the walls are nonconducting, the expressions for V and B , as given by Shercliff [3] can be written as

$$\begin{aligned} V &= \frac{1}{2}(\chi^2 - y^2) - \sum_{k=1}^{\infty} A_k \\ &\times \left(\frac{\text{sh } m_1 \text{ ch } m_2 x + \text{sh } m_2 \text{ ch } m_1 x}{\text{sh}(m_1 + m_2)} \right) \cos \omega_k y, \end{aligned} \quad (7)$$

$$\begin{aligned} B &= \sum_{k=1}^{\infty} A_k \\ &\times \left(\frac{\text{sh } m_1 \text{ sh } m_2 x - \text{sh } m_2 \text{ sh } m_1 x}{\text{sh}(m_1 + m_2)} \right) \cos \omega_k y \end{aligned} \quad (8)$$

where

$$m_1 = -\alpha + \mu_k, \quad m_2 = \alpha + \mu_k, \quad (9)$$

$$\mu_k = (\alpha^2 + \omega_k^2)^{1/2},$$

$$\omega_k = (2k - 1)\pi/2\chi, \quad (10)$$

$$A_k = \frac{16\chi^2}{\pi^3} \left[\frac{(-1)^{k+1}}{(2k - 1)^3} \right].$$

To solve equation (5) for θ , the above expressions for V and B are used as substitutions. This leads to a very

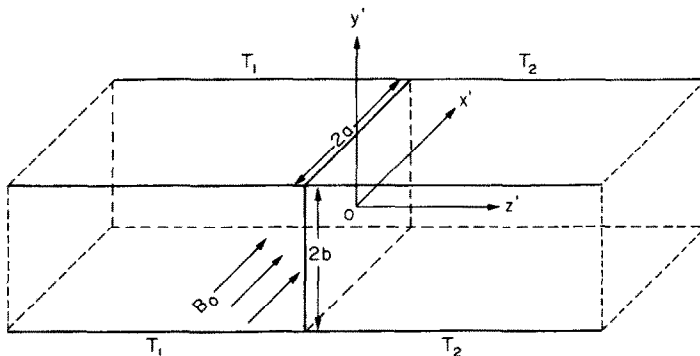


FIG. 1.

complicated RHS. The coefficient of $\partial\theta/\partial z$ is also variable. The analytical solution is therefore out of the question. To obtain the numerical solution, we have divided the discussion into two parts: (i) Solution for large $|z|$, and (ii) Solution near $z = 0$.

3. SOLUTIONS FOR LARGE VALUES OF $|z|$

As already pointed out, at large distances from the section $z = 0$, the effects of discontinuity will be negligible as a result of which the solution ceases to depend upon z ,

$$\theta(x, y, z) \rightarrow \Psi(x, y) \text{ as } z \rightarrow \infty. \quad (11)$$

The equation in Ψ can be obtained from equation (5) by replacing θ by Ψ and putting $\partial\theta/\partial z = 0$. This gives

$$\frac{\partial^2\Psi}{\partial x^2} + \frac{\partial^2\Psi}{\partial y^2} = -Q[(\nabla V)^2 + (\nabla B)^2] = -f(x, y) \quad (12)$$

The boundary conditions on Ψ will be

$$\begin{aligned} \Psi(\pm 1, y) &= 1, & |y| < \chi, & z < 0, \\ \Psi(x, \pm \chi) &= 1, & |x| < 1, & z < 0, \\ \Psi(\pm 1, y) &= 0, & |y| < \chi, & z > 0, \\ \Psi(x, \pm \chi) &= 0, & |x| < 1, & z > 0. \end{aligned} \quad (13)$$

Hereafter, we shall denote the solutions of equation (12) for $z \rightarrow -\infty$ and $z \rightarrow \infty$ by Ψ_1 and Ψ_2 , respectively. It is immediately clear that

$$\Psi_1(x, y) = 1 + \Psi_2(x, y). \quad (14)$$

Therefore we shall concentrate on finding Ψ_2 only.

3.1. Numerical solution of equation (12)

To solve the Dirichlet problem defined by equations (12) and (13), we have used the finite difference method. For this we have chosen the square pipe ($\chi = 1$) and

fitted a mesh of size $\Delta x = 1/8, \Delta y = 1/8$. This leads to 225 internal nodes in all in the entire section. However, owing to the symmetry about both axes, the discretization is done only in the first quadrant. Notice that this amounts to using the conditions $\partial\Psi_2/\partial x = 0$ and $\partial\Psi_2/\partial y = 0$ along $x = 0$ and $y = 0$, respectively. This leaves 64 unknowns. Counting i in x -direction and j along y -direction and denoting the value at the point (x_i, y_j) or $(i\Delta x, j\Delta y)$ by Ψ_{ij} , the discretization at (x_i, y_j) gives

$$\begin{aligned} \Psi_{i-1,j} + \Psi_{i+1,j} + \Psi_{i,j-1} + \Psi_{i,j+1} - 4\Psi_{ij} \\ = -h^2 f_{ij} + O(h^4) \end{aligned} \quad (15)$$

where

$$f_{ij} = f(x_i, y_j), \quad i = 1(1)8, \quad j = 1(1)8.$$

To compute f_{ij} , we first obtained the expressions for $\partial V/\partial x, \partial V/\partial y, \partial B/\partial x, \partial B/\partial y$ by differentiating equations (7) and (8) and then evaluated these numerically at all 64 points. The values of f_{ij} for different Hartmann numbers, with $Q = 1$, are obtained. The solution of the equations given by equation (15) is a quite simple task as the coefficient matrix is banded. The graphs showing $\Psi_2(x, y)$ along the x and y axes are plotted in Figs. 2 and 3. $\Psi_1(x, y)$ is then obtained from equation (13).

4. SOLUTION NEAR $z = 0$

Although the solution $\Psi_2(x, y)$ obtained above is valid only when $z \rightarrow \infty$, the perturbations due to the discontinuity at $z = 0$ have negligible effect after some distance, say $Z_2 > 0$, to the right of $z = 0$. Then $\Psi_2(x, y)$ gives a fairly good temperature distribution in the range (Z_2, ∞) . Similarly, $\Psi_1(x, y)$ is valid in the range $(-\infty, -Z_1)$, where $Z_1 > 0$ is some suitable number. Now the problem remains to solve equation (5) in the bounded region

$$-1 < x < 1, \quad -\chi < y < \chi, \quad -Z_1 < z < Z_2. \quad (16)$$

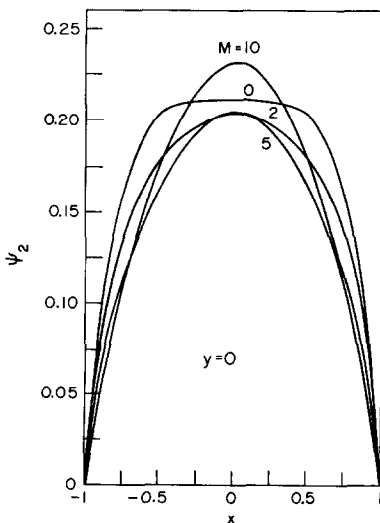


FIG. 2. Plot of Ψ_2 along x -axis.

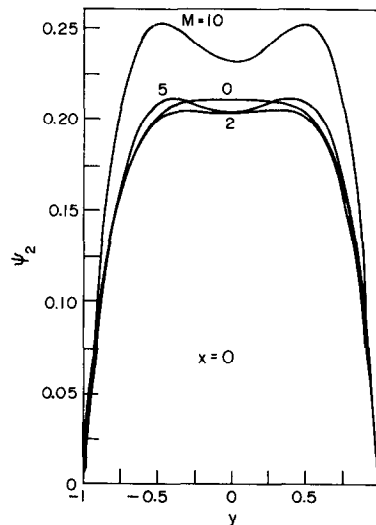


FIG. 3. Plot of Ψ_2 along y -axis.

The boundary conditions on θ will be

$$\begin{aligned} \theta(\pm 1, y, z) &= 1, \quad |y| < \chi, \quad -Z_1 \leq z < 0, \\ \theta(x, \pm \chi, z) &= 1, \quad |x| < 1, \quad -Z_1 \leq z < 0, \\ \theta(\pm 1, y, z) &= 0, \quad |y| < \chi, \quad 0 < z \leq Z_2, \\ \theta(x, \pm \chi, z) &= 0, \quad |x| < 1, \quad 0 < z \leq Z_2, \\ \theta(x, y, Z_1) &= \Psi_1(x, y), \quad |x| < 1, \quad |y| < \chi, \\ \theta(x, y, Z_2) &= \Psi_2(x, y), \quad |x| < 1, \quad |y| < \chi. \end{aligned} \tag{17}$$

4.1. ADI method

To solve the above 3-dim. problem in which $V(x, y)$ appears as a variable coefficient, we have applied the Peaceman-Rachford ADI method. For this purpose, we fit a mesh of size $\Delta x, \Delta y, \Delta z$ along the three axes. Let it give, say, I, J and K internal nodes along these directions. A point (x_i, y_j, z_k) in the region under consideration is defined by

$$\begin{aligned} x_i &= (i - 1) \Delta x - 1, \quad i = 1(1)I + 2, \\ y_j &= (j - 1) \Delta y - 1, \quad j = 1(1)J + 2, \\ z_k &= (k - 1) \Delta z - Z_1, \quad k = 1(1)K + 2, \end{aligned} \tag{18}$$

where $i = 1, I + 2; j = 1, J + 2; k = 1, K + 2$ correspond to the boundary points. We shall denote the value of θ at (x_i, y_j, z_k) by θ_{ijk} . For $\Delta x = \Delta y = \Delta z = h$, the Peaceman-Rachford scheme can be expressed by the following equations:

$$\begin{aligned} (\omega - \delta_x^2) \theta_{ijk}^* &= (\omega + \delta_y^2 + \beta^2 \delta_z^2 - hV_{ij\mu_z} \delta_z) \theta_{ijk}^n + h^2 f_{ij} \\ &= p_{ijk}^n, \quad \text{say, } i = 2(1)I + 1, \end{aligned} \tag{19}$$

$$\begin{aligned} (\omega - \delta_y^2) \theta_{ijk}^{**} &= (\omega + \delta_x^2 + \beta^2 \delta_z^2 - hV_{ij\mu_x} \delta_x) \theta_{ijk}^* + h^2 f_{ij} \\ &= p_{ijk}^*, \quad \text{say, } j = 2(1)J + 1, \end{aligned} \tag{20}$$

$$\begin{aligned} (\omega - \beta^2 \delta_z^2) \theta_{ijk}^{n+1} &= (\omega + \delta_x^2 + \delta_y^2 - hV_{ij\mu_z} \delta_z) \theta_{ijk}^{**} + h^2 f_{ij} \\ &= p_{ijk}^{**}, \quad \text{say, } k = 2(1)K + 1, \end{aligned} \tag{21}$$

where

$$\begin{aligned} \delta_x^2 \theta_{ijk} &= \theta_{i-1,j,k} - 2\theta_{ijk} + \theta_{i+1,j,k} \\ \mu_z \delta_z \theta_{ijk} &= \frac{1}{2}(\theta_{i,j,k+1} - \theta_{i,j,k-1}) \text{ etc.} \end{aligned} \tag{22}$$

and V_{ij} is the velocity at (x_i, y_j) which have been computed from the exact solution (7). Here $\omega > 0$ is a parameter to be suitably chosen to give fast convergence. The three steps above give values after $(n + 1)$ iterations starting from values at n^{th} iteration. The values with superscripts * and ** are intermediate values. The totality of the above scheme leads to the following matrix equations:

$$A_j \theta_{jk}^* = r_{jk}^n, \quad j = 2(1)J + 1, \quad k = 2(1)K + 1, \tag{23}$$

$$A_j \theta_{ik}^{**} = r_{ik}^*, \quad i = 2(1)I + 1, \quad k = 2(1)K + 1, \tag{24}$$

$$A_k' \theta_{ij}^{n+1} = r_{ij}^{**}, \quad i = 2(1)I + 1, \quad j = 2(1)J + 1, \tag{25}$$

where A_i and A_j are tridiagonal matrices of orders I and J , respectively, defined by

$$a_{ij} = 2 + \omega, \quad i = j,$$

$$\begin{aligned} &= -1, \quad |i - j| = 1, \\ &= 0, \quad \text{otherwise.} \end{aligned} \tag{26}$$

Similarly, the matrix A_k' is again a tridiagonal matrix of order K whose elements are defined by

$$\begin{aligned} a'_{ij} &= 2 + \omega/\beta^2, \quad i = j, \\ &= -1, \quad |i - j| = 1, \\ &= 0, \quad \text{otherwise.} \end{aligned} \tag{27}$$

The vectors θ and r are given by

$$\begin{aligned} \theta_{jk}^* &= [\theta_{2jk}^*, \theta_{3jk}^*, \dots, \theta_{(I+1)jk}^*]^T, \\ \theta_{ik}^{**} &= [\theta_{i2k}^{**}, \theta_{i3k}^{**}, \dots, \theta_{i(J+1)k}^{**}]^T, \\ \theta_{ij}^{n+1} &= [\theta_{ij2}^{n+1}, \theta_{ij3}^{n+1}, \dots, \theta_{ij(K+1)}^{n+1}]^T, \\ r_{jk}^n &= [p_{2jk}^n + \theta_{1jk}^*, p_{2jk}^n, \dots, p_{ijk}^n, p_{(i+1)jk}^n + \theta_{(i+2)jk}^*]^T \\ r_{ik}^* &= [p_{i2k}^* + \theta_{i1k}^*, p_{i3k}^*, \dots, p_{iJk}^*, p_{i(J+1)k}^* + \theta_{i(J+2)k}^*]^T, \\ r_{ij}^{**} &= [p_{ij2}^{**}/\beta^2 + \theta_{ij1}^{n+1}, p_{ij3}^{**}/\beta^2, \dots, p_{ijK}^{**}/\beta^2, \\ &\quad p_{ij(K+1)}^{**}/\beta^2 + \theta_{ij(K+2)}^{n+1}]^T. \end{aligned} \tag{28}$$

Each one the matrices A_i, A_j and A_k' is tridiagonal and diagonally dominant. The solution can be obtained using the Thomas algorithm [5] or still better using the Evans decomposition [6].

Notice that by solving equation (23) all the unknowns which are IJK in number, are being obtained at the * level by solving only I tridiagonal equations at a time, line by line where lines are being taken parallel to the x -axis. Similarly, equation (24) requires solution of only J equations at a time by taking lines parallel to the y -axis. This gives all unknowns at the ** level. Finally, from equation (25) we determine all the unknowns at the $(n + 1)$ level by solving K equations at a time. It has been found that the total number of operations (multiplication and division) required in going from the n th to the $(n + 1)$ th iterations is

$$6IJK - (IJ + IK + JK)$$

where the unknowns involved will be $3IJK$. Keeping in view the other methods, e.g. Gaussian elimination, this is much more economical and efficient.

To start the iterations, the initial values are taken as

$$\begin{aligned} \theta_{ijk}^0 &= 1.0, \quad -Z_1 < z_k < 0, \quad i = 2(1)I + 1, \\ &= 0.5, \quad z_k = 0, \quad j = 2(1)J + 1, \\ &= 0.0, \quad 0 < z_k < Z_2. \end{aligned} \tag{30}$$

5. NUMERICAL WORK AND DISCUSSION

For all calculations, we have chosen $\chi = 1$, i.e. the section of the channel is a square of side 2. The values of β and Q are also chosen as unity. The mesh size is taken as $\Delta x = \Delta y = \Delta z = h = 1/8$. This gives $I = J = 15$. The values $Z_1 = Z_2 = 4.0$ are obtained by trial and error because we have noted that the perturbations in θ due to discontinuity at $z = 0$ are negligible outside

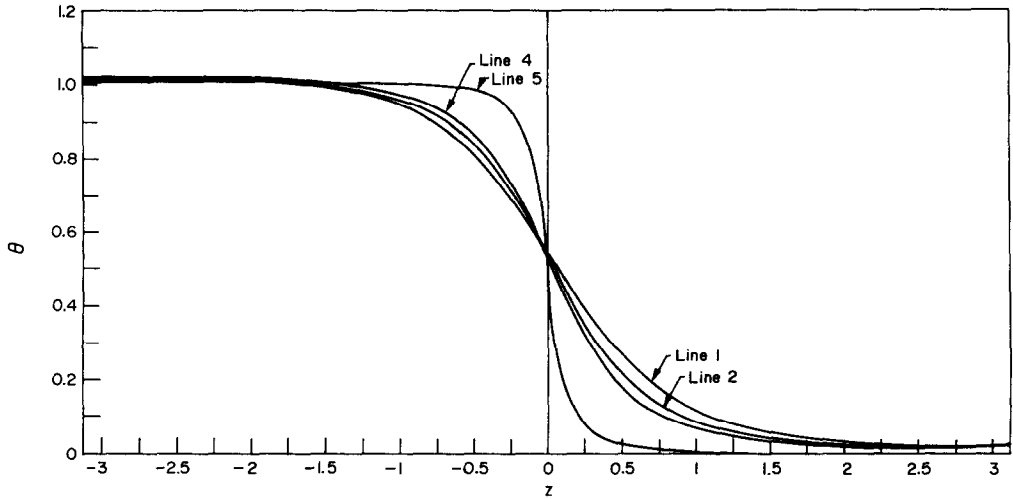


FIG. 4. Temperature distribution on lines 1, 2, 4 and 5 for $M = 5$.

$[-4, 4]$. This, with $h = 1/8$, gives $K = 63$. The choice $\beta = 1$ has an advantage that the diagonal elements in all the matrices A_j , A_j and A'_k have the same numerical values and the same decomposition will work for all of them. The parameter ω is again obtained by trial and error. We found $\omega = 4.7$ leads to a very fast convergence. Note more than 80 iterations were required for any Hartmann number. Actually, in some cases, only 30 iterations were needed to achieve 5-place accuracy. The choice of the initial values is also important but in the present circumstances we did not

have a better choice than given by equations (30). It was also noticed that one cycle of iterations took about 2 s of CPU time on a DEC-2050 system.

The calculations were carried out for the temperature distribution at 4160 points given by

$$\begin{aligned} x_i &= i/8, & i &= 1(1)8, \\ y_j &= j/8, & j &= 1(1)8, \\ z_k &= -4 + (k - 1)/8, & k &= 1(1)65, \end{aligned} \quad (31)$$

for various values of the Hartmann number. We have

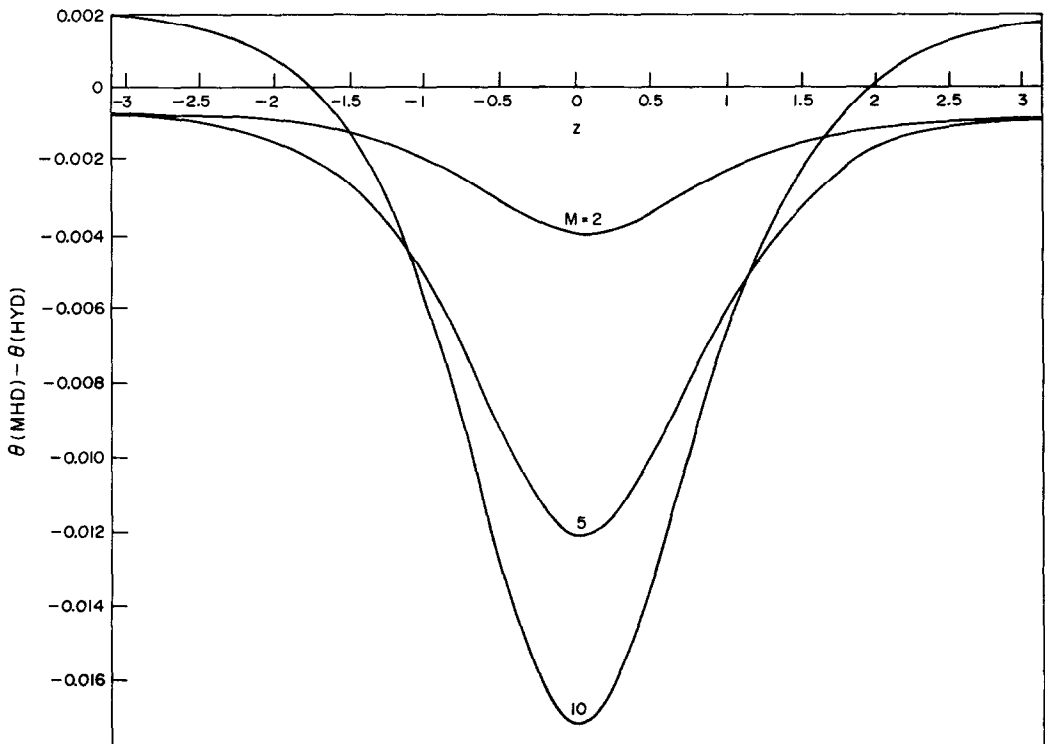


FIG. 5. Temperature difference between MHD and hydrodynamic cases on line 1.

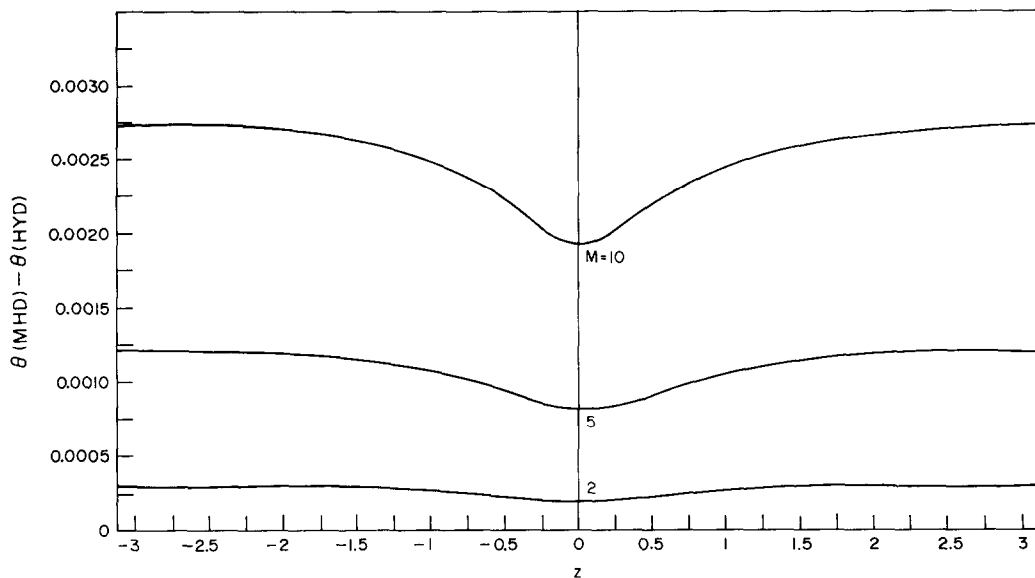


FIG. 6. Temperature difference between MHD and hydrodynamic cases on line 5.

chosen following lines for the discussion of the results:

$$\left. \begin{array}{l} 1. x = 0, \quad y = 0 \\ 2. x = 1/2, \quad y = 0 \\ 3. x = 0, \quad y = 1/2 \\ 4. x = 1/2, \quad y = 1/2 \\ 5. x = 7/8, \quad y = 7/8 \end{array} \right\} -4 \leq z \leq 4. \quad (32)$$

Figure 4 gives the variation of θ along the lines 1, 2, 4 and 5 for $M = 5$ (line 3 is not depicted due to the overlapping of graphs). After examining several graphs, which include those for the difference between MHD and hydrodynamic cases along several lines for various Hartmann numbers, we have made the following observations:

(1) In the presence of a magnetic field the temperature shows a decreasing tendency in the region close to the discontinuity. This effect becomes more and more pronounced as the Hartmann number increases (Fig. 5).

(2) Away from the discontinuity, the temperature shows increasing tendency with Hartmann number (Fig. 5).

(3) The lines very close to the boundary are an exception as shown in Fig. 6 where temperature increases with Hartmann number for all values of z . This is due to the high electric currents following in the boundary layers giving larger heating effects.

REFERENCES

1. S. D. Nigam and S. N. Singh, Heat transfer by laminar flow between parallel plates under the action of a transverse magnetic field, *Q. J. Mech. Appl. Maths.* **13**, 85-96 (1960).
2. B. Singh and J. Lal, Temperature distribution for MHD flow between coaxial cylinders with discontinuity in wall temperatures, *Appl. Sci. Res.* **35**, 67-83 (1979).
3. J. A. Shercliff, Steady motion of conducting fluids in pipes under transverse magnetic fields, *Proc. Camb. Phil. Soc.* **49**, 136-144 (1953).
4. D. W. Peaceman and H. H. Rachford, The numerical solution of parabolic and elliptic differential equations, *J. Soc. Ind. Appl. Math.* **3**, 28-41 (1955).
5. L. H. Thomas, Elliptic problems in linear difference equations over a network, Watson Scientific Computing Lab., Columbia University, New York (1949).
6. D. J. Evans, An algorithm for the solution of certain tridiagonal systems of linear equations, *Comput. J.* **15**, 356-359 (1972).

TRANSFERT THERMIQUE POUR UN ECOULEMENT MHD A TRAVERS UN TUBE RECTANGULAIRE AVEC DISCONTINUITÉ DES TEMPERATURES DE PAROI

Résumé—On étudie numériquement la distribution de température d'un écoulement permanent axial MHD à travers un tube rectangulaire. Du fait de la discontinuité des températures de paroi, l'équation aux dérivées partielles est elliptique, à trois dimensions, avec des coefficients variables et elle ne peut être résolue analytiquement. Les méthodes classiques aux différences finies ne sont pas adaptées à cause du grand nombre d'inconnues impliquées. La méthode ADI est la plus adaptée car elle économise du temps de calcul et des mémoires de l'ordinateur. On donne des graphes pour représenter la distribution de température près et en aval de la discontinuité, pour différents nombres de Hartmann.

**WÄRMEÜBERTRAGUNG AN EINE MHD-STRÖMUNG IN EINEM RECHTECKIGEN ROHR
MIT VERÄNDERLICHEN WANDTEMPERATUREN**

Zusammenfassung—Die Temperaturverteilung in einer stationären axialen MHD-Strömung in einem rechteckigen Rohr wurde numerisch berechnet. Wegen der Diskontinuität der Wandtemperaturen kann die resultierende Differentialgleichung, eine dreidimensionale elliptische partielle Differentialgleichung mit veränderlichen Koeffizienten, nicht analytisch gelöst werden. Das traditionelle Differenzenverfahren läßt sich infolge der großen Zahl der enthaltenen Unbekannten nicht anwenden. Das ADI-Verfahren, so wird festgestellt, ist das geeignetste Verfahren zur Lösung dieses Problems, da es sowohl Rechenzeit als auch Speicherplatz spart. Anhand von grafischen Darstellungen wird die Temperaturverteilung an und in einiger Entfernung von der Diskontinuität bei verschiedenen Hartmann-Zahlen gezeigt.

**ТЕПЛОПЕРЕНОС ПРИ МГД-ТЕЧЕНИИ В ПРЯМОУГОЛЬНОМ КАНАЛЕ СО
СКАЧКОМ В РАСПРЕДЕЛЕНИИ ТЕМПЕРАТУРЫ СТЕНОК**

Аннотация—Численным методом получено распределение температур для стационарного аксиального МГД-течения в прямоугольном канале. Из-за скачка в распределении температуры стенок полученное дифференциальное уравнение, представляющее собой трехмерное эллиптическое уравнение в частных производных с переменными коэффициентами, невозможно решить аналитически. Традиционные разностные методы оказались непригодными из-за очень большого числа неизвестных. Найдено, что наиболее подходящим является неявный метод переменных направлений, позволяющий экономить время и память компьютера. Представлены кривые распределения температур вблизи и вдали от скачка температуры при различных значениях числа Гартмана.